Power Loss and Optimised MOSFET Selection in BLDC Motor Inverter Designs

Understanding MOSFET power losses in block (trapezoidal) commutation

Author:

Elvir Kahrimanovic

Senior Application System Engineer

Elvir.Kahrimanovic@infineon.com

Abstract

Brushless DC (BLDC) motors offer a number of advantages in applications including medical equipment, home appliances, cordless power tools and industrial automation. Among the challenges facing designers of BLDC motor applications is the delivery of optimum efficiency for a given price/performance point.

Achieving the best solution means knowing how to choose the most appropriate MOSFETs. A common practice for designers evaluating the power stage is to measure the temperature and correlate the power losses with the temperature measurement, but this only provides the overall power losses. The lack of detailed information on power losses makes a good design very difficult.

In this whitepaper, Infineon Technologies looks at the challenges facing designers of BLDC motor inverters using block (trapezoidal) commutation and factors to consider relating to MOSFET selection - including accurate identification of relevant losses in the power stage.

Contents

1 Brushless DC Motors

From cordless power tools to industrial automation and from electric bikes to remote-controlled ‘drones’, an increasing number of motion control applications are now being built around the brushless DC (BLDC) motor. While BLDC solutions require more complex drive electronics than brushed alternatives, these motors offer a number of operational advantages that include higher efficiency and higher power density. This allows smaller, lighter and less expensive motors to be deployed. At the same time, there is less mechanical wear-and-tear, which leads to higher reliability, longer lifetimes and eliminates need for ongoing maintenance. BLDC motors also operate with lower audible and electrical noise than their brushed counterparts.

Sometimes referred to as an electronically commutated motor (ECM), a typical BLDC motor has a three-phase stator which keeps turning the rotor via an electronic control scheme that incorporates a three-phase inverter circuit. This circuit continually switches currents in the stator windings in synch with the rotor position which can be ascertained via sensors or through calculations based on the back electromotive force (EMF) at any particular moment. The flux generated in the stator interacts with the rotor flux, which defines the torque and the speed of the motor.

When designing a BLDC application, engineers can choose between using discrete components or integrated semiconductors that bring together a number of important drive and control functionalities into a single device. In this white paper we consider a BLDC motor application that has been built using discrete components. In this case the key functional blocks comprise power management, digital control, drivers and a three-phase inverter as shown in Figure 1.

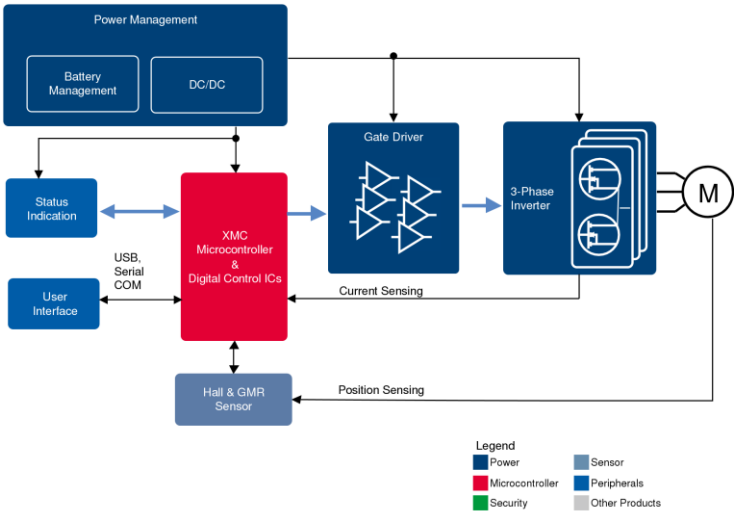

Figure 1: Example application for brushless DC motor with discrete components

Figure 2 shows in detail an inverter stage used to drive a 3-phase BLDC motor in a common block (trapezoidal) commutation control scheme. The motor is typically equipped with Hall switches offering '1' or '0' outputs that feedback rotor position to the host microcontroller. These switches are necessary for applications such as cordless power drills where the motor needs to provide a high torque at or near zero speed.

The stage comprises three half bridges (one half bridge for each motor terminal) made up of high-side (HS) MOSFETs (Q1, Q2 and Q3) and low-side (LS) MOSFETs (Q4, Q5 and Q6). The average voltage of the output of each half bridge is regulated between 0 V and V_{DC} through the application of a pulse width modulated (PWM) signal to the HS and LS MOSFETs. This signal is generated by the host microcontroller and delivered to the MOSFETs via the gate drive ICs.

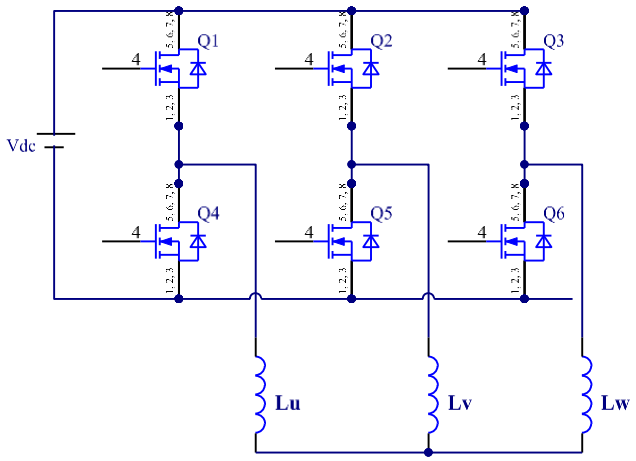

Figure 2: Power inverter stage

Gaining a true understanding of the losses incurred during the operation of the power inverter stage is fundamental in addressing rugged and cost efficient design requirements. And while, accurately calculating such power loss is not a trivial exercise, with the right measurements, support and tools it can be done very effectively.

2 Block (Trapezoidal) Commutation

In a block commutation scheme there are six distinctive modes of operation. Table 1 provides the sequence of active power devices during a specific block (refer to figure 2.), while Figure 3 shows the corresponding phase current waveforms based on 100% duty cycle.

Commutation table				
BLOCK	HS MOSFET	LS MOSFET	Sync MOSFET	Hall patterns
I	S1	S5	S4	101
II	S3	S5	S6	100
III	S3	S4	S6	110
IV	S2	S4	S5	010
V	S2	S6	S5	011
VI	S1	S6	S4	001

Table 1: Active power devices in a block commutation scheme

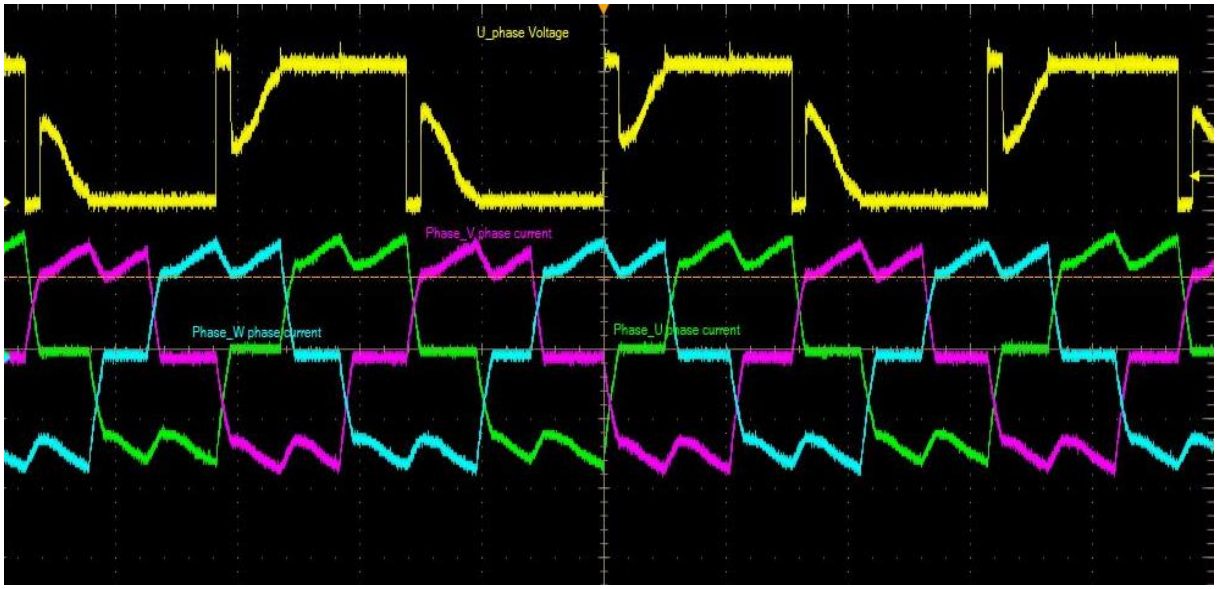

Figure 3: Phase voltage and current waveforms of a 3-phase inverter in block commutation BLDC motor at 100% duty cycle.

Let’s consider further how the phase voltage and phase current relate to each other.
In Figure 4 we identify 3-phase voltage marked as V_u, V_v, V_w (green traces) and the corresponding phase currents as I_u, I_v, I_w (red traces) and note the phase separation of 120 electrical degrees between these signals. The blue trace drafted around V_u signal would indicate 100% duty cycle.
The hall sensor signals are generated by hall switches integrated within the motor mechanical structure and are used by the microcontroller to trigger and apply the correct voltage on the appropriate phase.

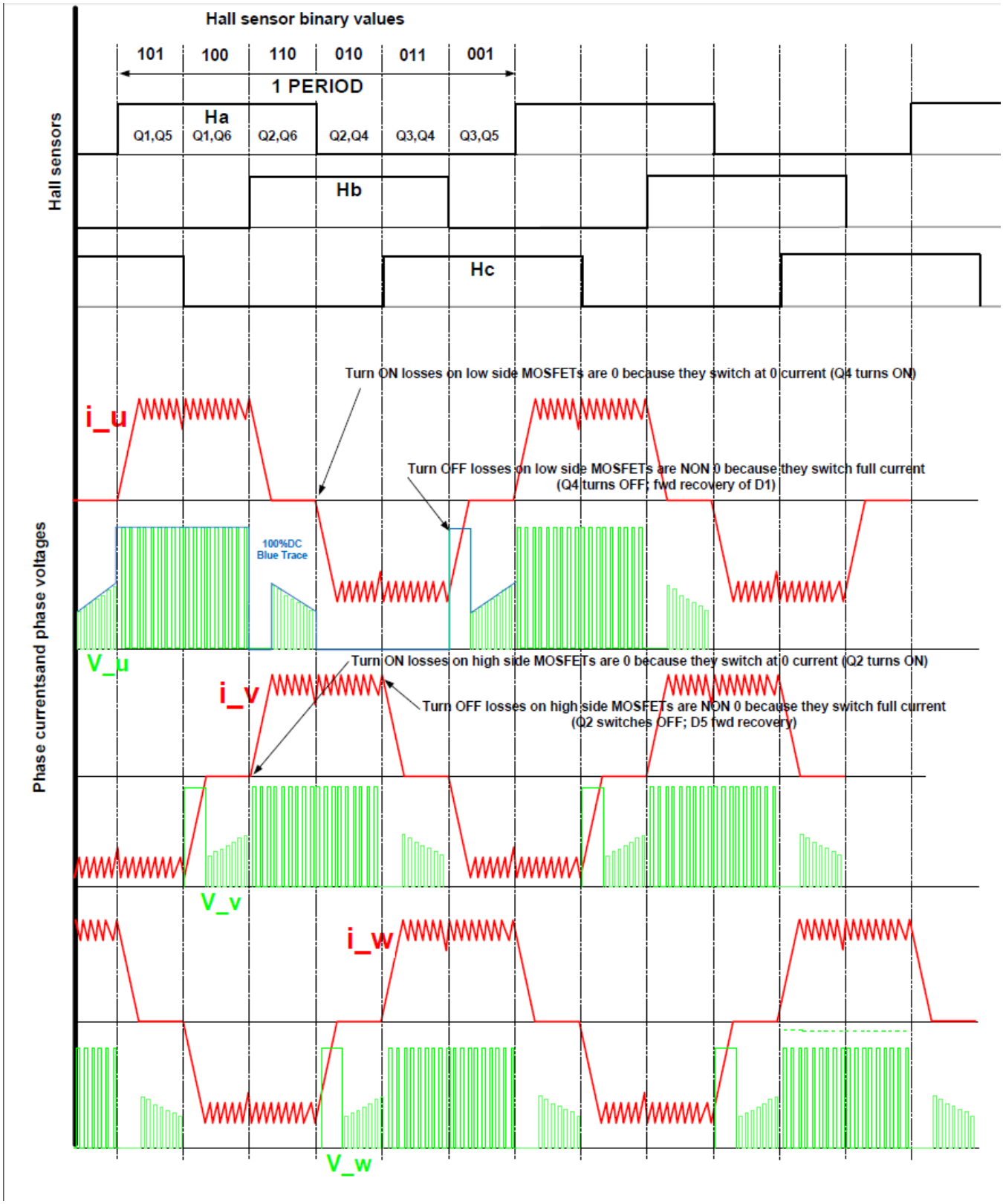

Figure 4: Phase currents and phase voltages in block commutation

3 Analysis of a 3-phase current waveform

In a block commutation BLDC motor drive, a typical phase current is that shown in Figure 5a and 5b.

Figure 5: Phase current at 100% and 50% duty cycle

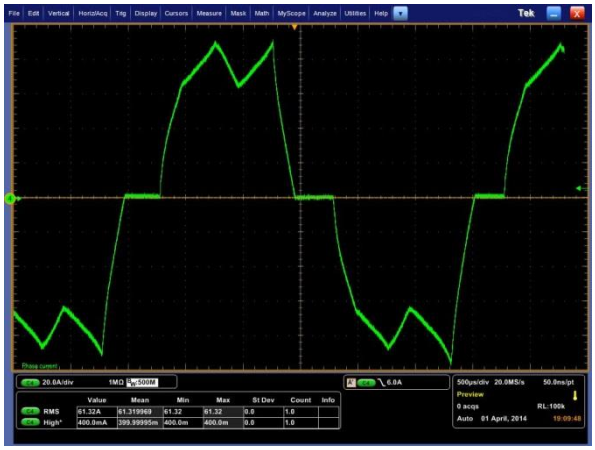

Figure 5a: Phase current at 100% duty cycle

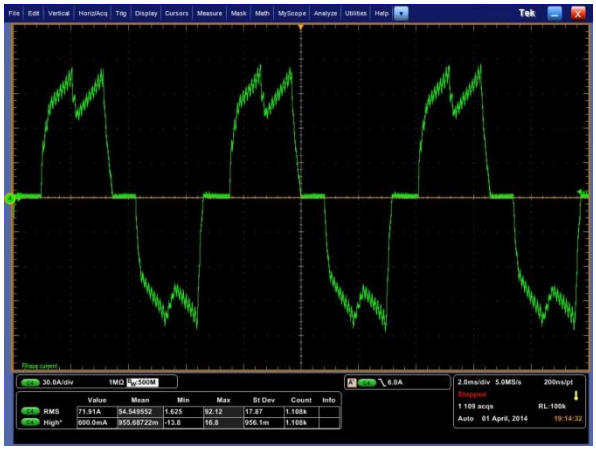

Figure 5b: Phase current at 50% duty cycle (note current ripples at switching frequency of 10 kHz)

By analysing the waveform in terms of switching patterns and the switching devices conducting this current, the phase current waveform provides almost all the necessary information needed to calculate different losses in the MOSFET.

So let’s have a closer look at the current waveform as shown in Figure 6.

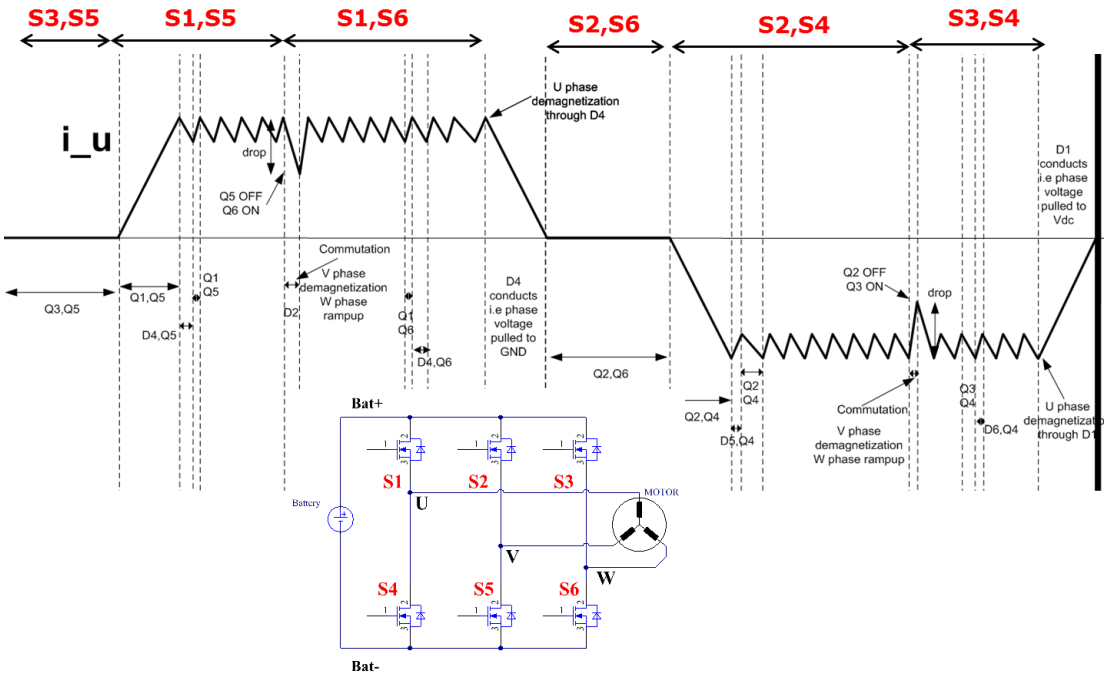

Figure 6: Phase current

The diagram shows the details of the phase current flowing in the U phase of the motor for the duration of one electrical period. This period is related to the speed of the motor by the number of poles. The faster the motor rotates, the shorter the period. In a high-speed motor running at about 20,000 rpm and having two pole pairs the electrical period can be calculated as:

$$T_{electrical} = \frac{60}{\text{2 pole pairs x motor speed}} = \frac{60}{\text{2 x 20,000}} * 1.5\ ms \rightarrow f_{electrical} = 666\ Hz$$

This frequency should not be confused with the switching frequency, which is commonly chosen between 10 kHz – 20 kHz to reduce current ripples and or audible noise.

3.1 Circuit analysis of B6 inverter in block cummutation

Block 1: S1, S5

To control the speed of the motor we need to reduce the voltage across the motor winding. To achieve this we apply PWM pulses to MOSFET S1 while we keep S5 turned ON (unipolar voltage switching).

When S1 turns ON, the current in phase winding U and V ramps up. When S1 turns OFF, the current through windings U and V continues through Diode D4 (the internal MOSFET diode). In order to reduce losses in this diode we turn on the MOSFET S4 so that, instead of diode power loss which is calculated as V*I, we have $I^2 * R_{DS(on)}$ losses. In general these MOSFETs conduction power losses are much lower than diode power losses.

Before we turn ON the low side MOSFET S4 we need to ensure that the high side MOSFET S1 is completely turned off, otherwise we would have a shoot through condition where both high and low side MOSFETs are turned on thereby shorting the battery. In order to prevent this we ensure some delay between high side MOSFET turn OFF and low side MOSFET turn ON. This time is also known as dead time and it varies depending on switching speed.

Before the high side MOSFETs can turn on again, we need to switch OFF the low side MOSFET. When the low side MOSFET turns off, we again need to allow some dead time before we switch ON the high side MOSFET. During this dead time D4 conducts again.

This process repeats until the microcontroller receives the signal from the hall sensors to commutate the phases because the rotor of the motor has advanced.

Block 2: S1, S6

Now switch S5 turn OFF and S6 turns ON. When S5 turns OFF, the current in V_{phase} decays through D2, thereby pulling the V_{phase} voltage to battery potential. This is also described as phase demagnetization of the motor winding V. The PWM pulses are again applied to S1 and when S1 turns off, the diode D4 is conducting (as well as S4 when synchronous rectification is applied). Note that the graph in Figure 6 does not show the synchronous rectification case.

In principle every switching cycle looks like that shown in Figure 7.

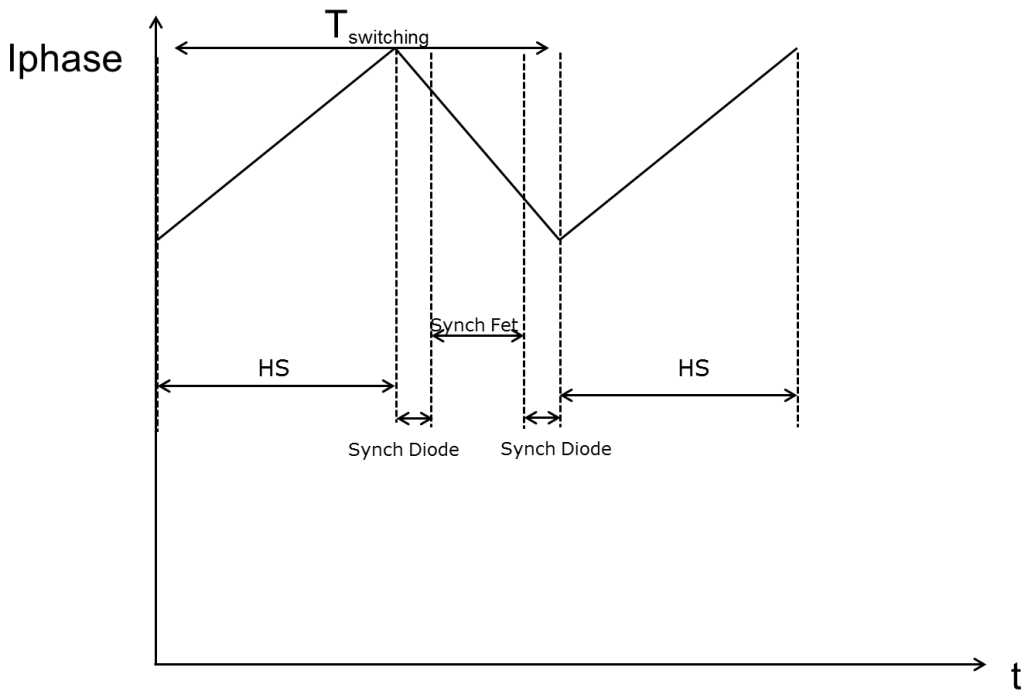

Figure 7: Switching cycle

When the microcontroller receives the commutation hall sensor signal from the motor, the S1 switch is turned OFF. Due to the inductance of the motor coil, the current has to continue in the same direction thereby forcing the diode D4 to conduct. The phase voltage is clamped to ground by D4 and will have the magnitude of the diode forward voltage drop (approx. -0.7 V).

Block 3: S2, S6 - OFF time

In this time the phase U is OFF since S2 and S6 are conducting and no current is established in the motor phase U.

Block 4: S2, S4

When the rotor advances further in its rotation, it triggers the hall sensor combination 010, which commands the MCU to turn ON S4 and apply PWM pulses to S2. The analysis follows the same analogy as in the BLOCK 1. The only difference is that the current is flowing in the negative direction. When S2 turns OFF, the demagnetization of the phase V is achieved with the diode D5 indicating the end of block 4.

Block 5: S3, S4

The current flow in phase U continues through the switch S3, which receives the PWM pulses and operates as long as the MCU doesn't receive the command to commutate phases. When S4 turns OFF, the demagnetization of the U phase is achieved with the diode D1 and the phase voltage is pulled to V_{bat} through D1.

Block 6: S3, S5 - OFF time

Once again we have no current flow in the phase U since S3 and S5 excite the current in the phases V and W. The end of Block 6 represents one full electrical period.

This electrical period can repeat several times during one full motor rotation of 360 degrees depending on number of rotor poles.

4 Power loss calculation in 3-phase inverter

In a 3-phase motor inverter the power dissipation consists of conduction, switching and diode losses. In order to choose the best price/performance MOSFET, an understanding of the split of these losses is necessary.

4.1 Conduction loss

During the ON time, the MOSFET behaves like a resistor and the conduction losses can be simply obtained by applying the formula:

$$P_{d,conduction} = {I_{rms}}^2 * R_{DS(on)}$$

Integration of the instantaneous power losses over the switching cycle gives an average value of the MOSFET conduction losses:

$$P_{CM} = \frac{1}{T_{sw}} \int_0^{Tsw} p_{CM}(t)dt = \frac{1}{T_{sw}} \int_0^{Tsw} (R_{DSon} \cdot i_D^2(t))dt = R_{DSon} \cdot I_{Drms}^2$$

Where I_{Drms} is the RMS value of the MOSFET on-state current.

We should not forget that MOSFET $R_{DS(on)}$ depends on temperature (see Figure 8).

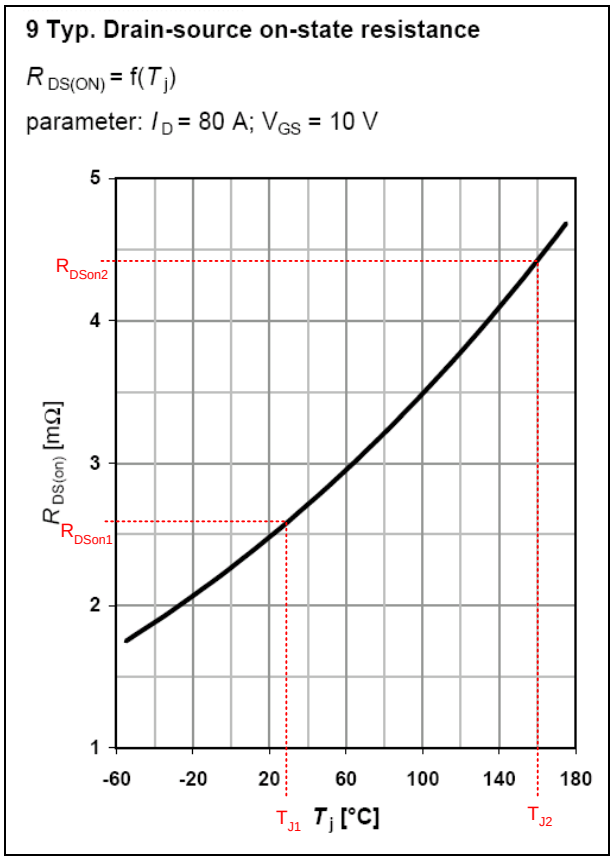

Figure 8: MOSFET $\boldsymbol{R_{DS(on)}}$ is temperature-dependent
Ref.1

Therefore before we can calculate the conduction power loss, we have to factor in the temperature.

$$R_{DSon}(T_J) = R_{DSonMAX}(25^{\circ}C) \cdot \left(1 + \frac{\alpha}{100}\right)^{T_J - 25°C}$$

Where T_J is the junction temperature and $R_{DS(on),max}$ (25 °C) is the maximum value of $R_{DS(on)}$ at 25 °C.

4.2 Switching loss

For the engineering calculations of the power loss balance, a linear approximation of the MOSFET switching process is sufficient. The idealised power MOSFET switching process is presented in Figure 9 below. The uppermost part (A) presents the gate voltage (U_{GS}) and current (i_G); the next one (B) shows the drain-source voltage (U_{DS}) and the drain current (i_D) without taking the reverse recovery of the free-wheeling diode into account. Part C gives a qualitative overview of the power loses, while part D shows the reverse-recovery effects on the switching losses.

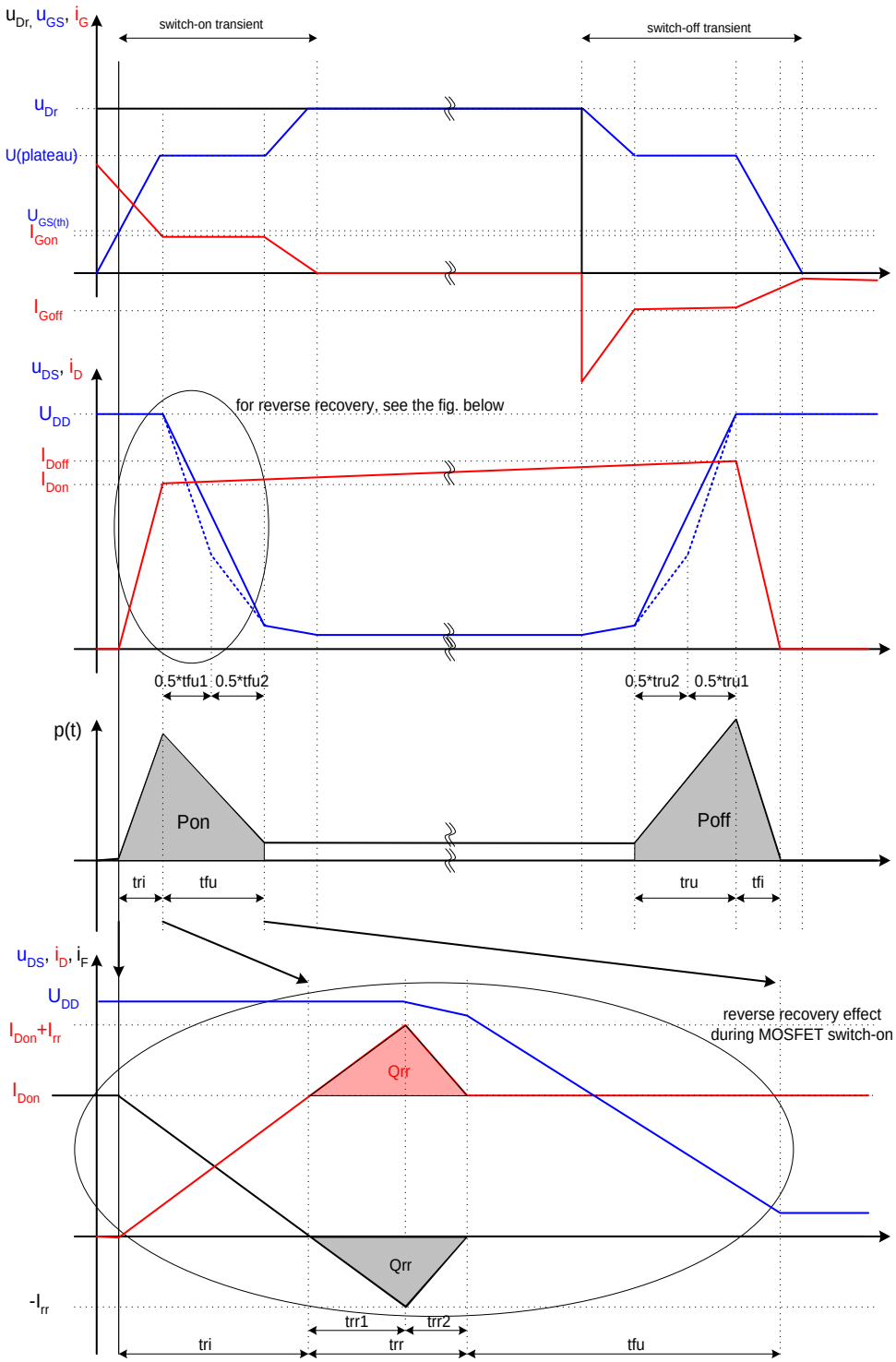

Figure 9: Idealized MOSFET switching process
Ref.1

Linearization of the MOSFET switching process is sufficient for good accuracy. Losses due to the reverse recovery charge of the intrinsic diode (Q_{rr} loss) at typical operating conditions of f_sw=10 kHz and taking into account a generally small Q_{rr} for low-voltage MOSFETs are small and will be omitted.

The switching loss is calculated by using the following method:

1. Obtain the duration of switching transition for switch ON and switch OFF
2. Multiply V_{DS} and I_d by this duration to obtain the single switching transition energy
3. Obtain the number of switching transitions in a single electrical period of the motor
4. Multiply the single switching transition energy by the number of switching transitions to obtain the total switching loss
5. Repeat the steps above for turn ON and turn OFF to separate these two types of losses

First, therefore, we have to find out how long the transition is and how many of these transitions we have in an electrical period (note that switching frequency has no relation to motor electrical period, which is related to mechanical rotation by number of poles).

We start by ascertaining the gate drive current for turn ON and turn OFF:

$$I_{g,on} = \frac{V_{gs-}V_{pl}}{R_{total\_gate}} \text{ ; turn ON}$$

$$I_{g,off} = \frac{V_{pl}}{R_{total\_gate}} \text{ ; turn OFF}$$

Where

V_{gs} *- gate driver voltage*

V_{pl} *- plateau voltage*

R_{total_gate} *- total gate resistance consisting of gate resistor and internal gate driver resistance*

Now we can obtain the duration of plateau voltage

$$t_{platueau\_ON} = \frac{Q_{g\_sw}}{I_{g,on}}$$

$$t_{platueau\_OFF} = \frac{Q_{g\_sw}}{I_{g,off}}$$

4.3 Diode loss

The MOSFET's intrinsic diode will have two different modes of operation.
If synchronous rectification is used the diode conducts only for the duration of dead time before and after MOSFET turns ON and OFF.

The other operating mode of the diode is phase demagnetization. This is the mode that occurs during each phase commutation.

5 Analysis of the 3-phase inverter losses in block commutation

Since the phase current waveform is symmetrical along the X-axis we can simplify the power loss analysis by analysing only the positive half of the waveform.

In the schematic of Figure 10 we can identify three MOSFETs that are operating during the positive part of the phase current waveform

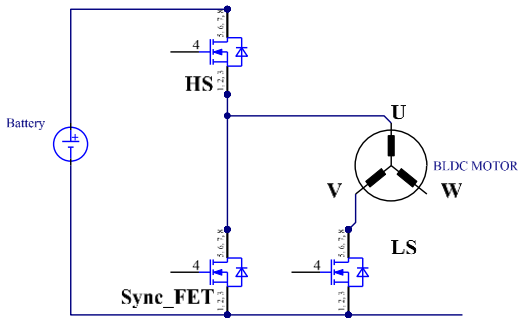

Figure 10: Active MOSFETs during positive part of the U phase current waveform

During a single block the low side MOSFET (LS) will be ON while on the high side MOSFET (HS) we apply PWM pulses. When the HS turns ON the current rises in the U and V phase. When the HS FET turns OFF, the current will initially flow through the diode of the SynchFET for the duration of the pre-programmed dead time, after which the SynchFET turns on to reduce the diode losses. Before the HS FET can turn ON, the low side FET has to turn OFF. When the LS FET turns OFF, the SynchFET diode will conduct again for the duration of the preprogramed dead time. Then HS turns on again. The frequency is usually in the range of 10-20 kHz depending on desired phase current ripple and audible noise. This should not be confused with

the phase commutation frequency, which is related to the motor speed and can be calculated by the formula:

$$Motor\ rpm = \frac{commutation\ frequency\ in\ Hz * 60}{number\ of\ pole\ pairs}$$

Since we analysed the operation of the BLDC motor in block commutation we can apply that knowledge to calculate the MOSFET losses.

A single-phase current waveform is sufficient to extract almost all necessary information for this calculation and to identify the power loss breakdown as shown in Figure 11.

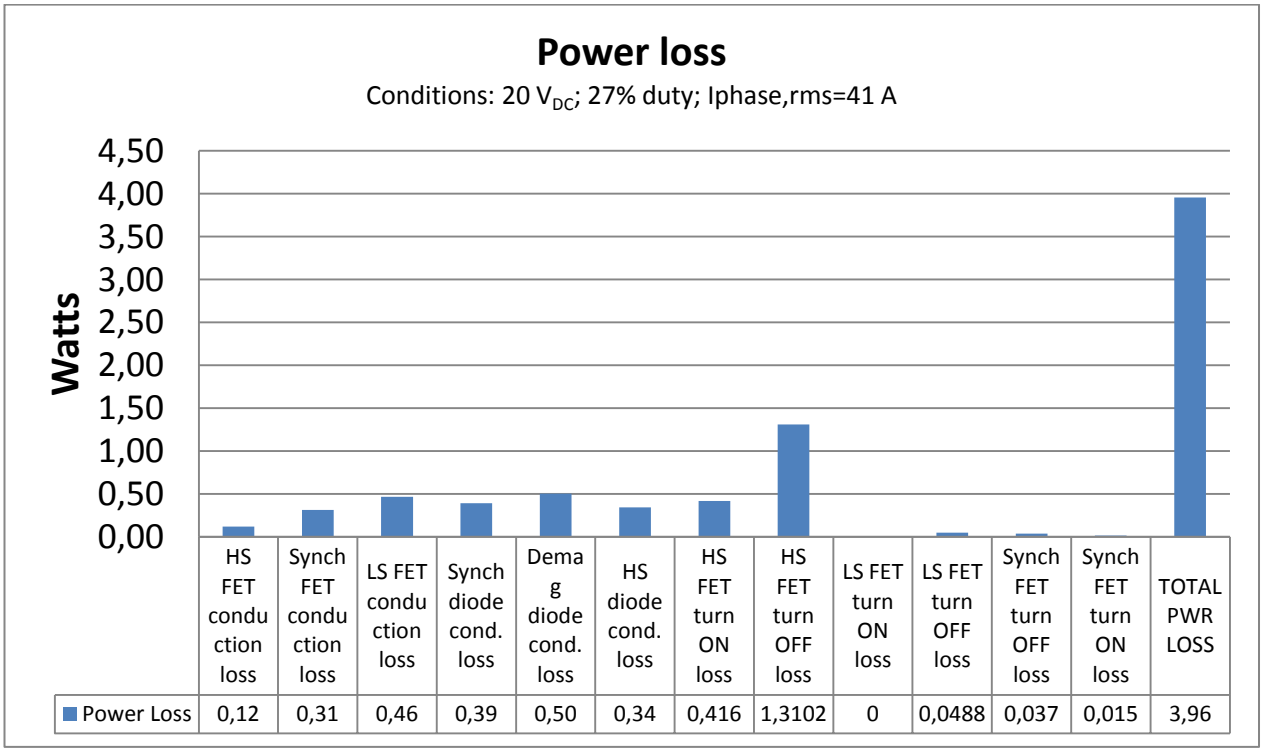

Figure 11: Power loss breakdown

We can also lump together these losses as shown in Figure 12:

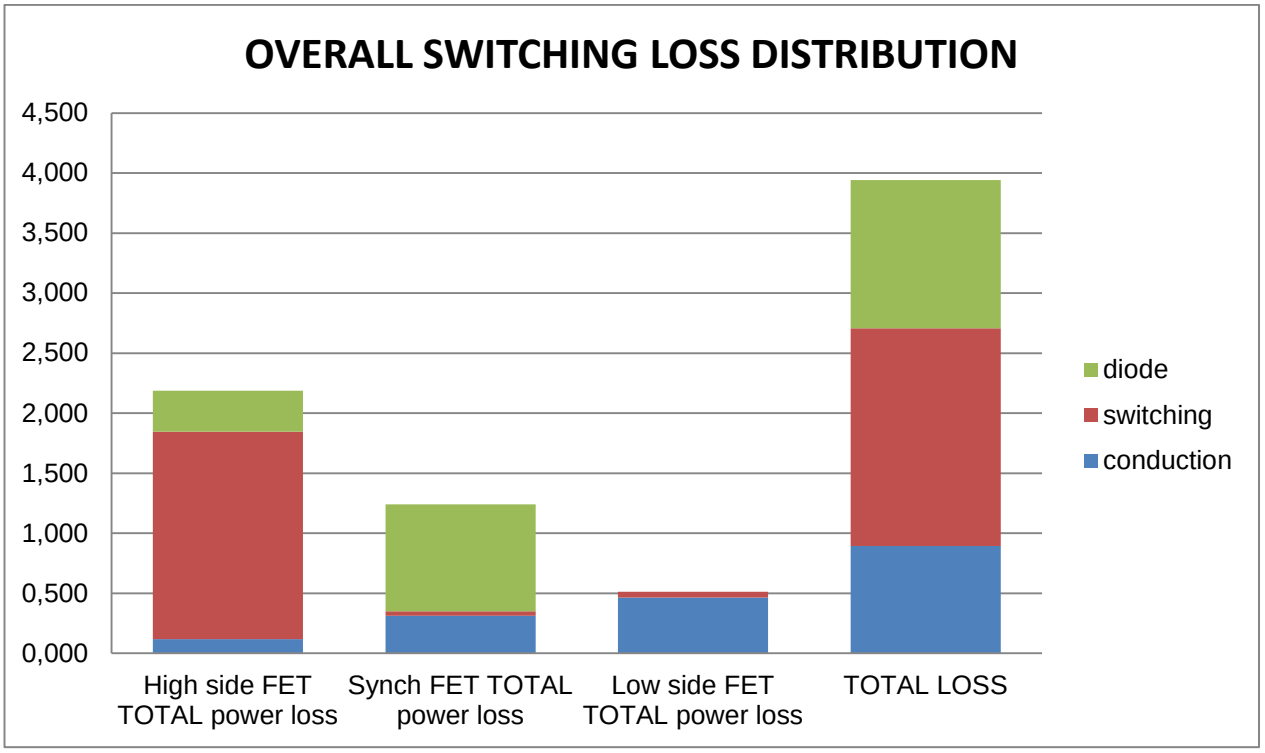

Figure 12: Overall loss breakdown

We can also look at the power dissipation from the single half bridge perspective (Figure 13)

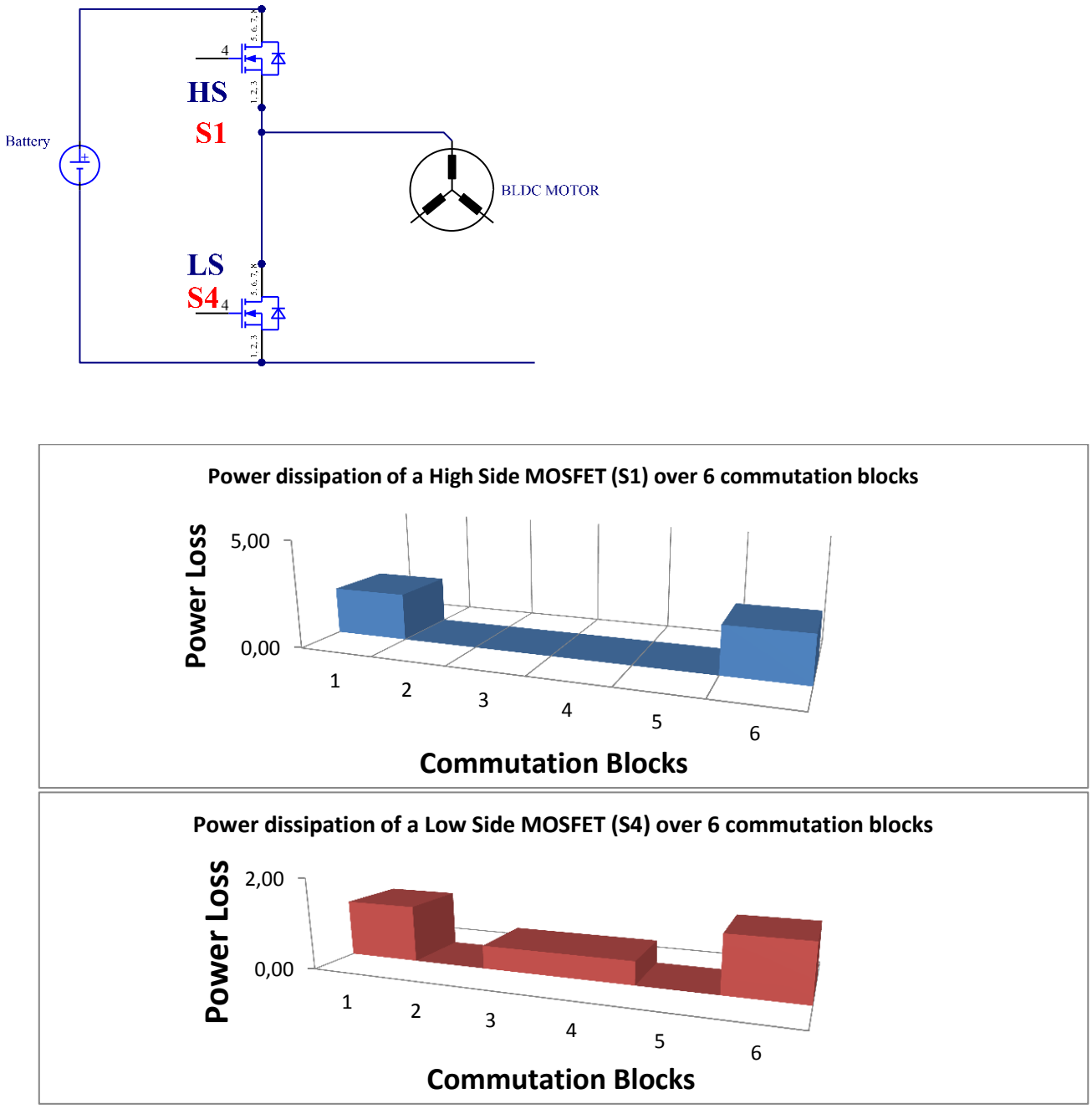

Figure 13: Instantaneous power dissipation in a single half bridge

By using this method we are able to get a better picture of power losses and, therefore, make an informed decision about the best price/performance MOSFET. Note that this is an instantaneous power dissipation which causes instantaneous heat on silicon die and cannot be measured by thermal camera or thermal probe.

By knowing this peak power, i.e. heat, one can ensure a reliable MOSFET operation.

This is done by multiplying the total MOSFET power loss by the cost of the MOSFET to give the best price performance ratio (lowest number).

Furthermore, when R_{th} and Z_{th} of the thermal system is known, it is easy to calculate whether the junction temperature of the MOSFET is exceeded in a desired condition (for example motor stall condition).

6 Example: Analysis of calculated power losses for cordless power drill motor

As an example, let us look and analyse the calculation results of power losses based on a test performed using a power drill motor in conjunction with the Infineon 1 kW BLDC power demo kit.

Test conditions:

V_{bat} = 20 V
I_{phase} = 42 A_{RMS}
Duty cycle = 27%
MOSFET: 2 x Infineon BSC 010N04LSI in parallel, each with integrated Schottky-like diode
Gate driver: 2EDL05N06
Gate resistors: 100 ohm per MOSFET

In this condition the dominant losses are switching losses. This is not surprising considering the fact that we are using 100 ohm gate resistors, but we notice that diode losses are higher than conduction losses. This means that the reduction of diode forward voltage drop rather than a lower $R_{DS(on)}$ will give us the greater benefits in our efforts to reduce power losses. The Infineon Schottky-like diode MOSFETs have lower diode voltage drop V_{fd}, and therefore can reduce the overall losses.

In the above example we considered only one condition at 27% duty cycle.
Below is the breakdown of several duty cycles and different currents

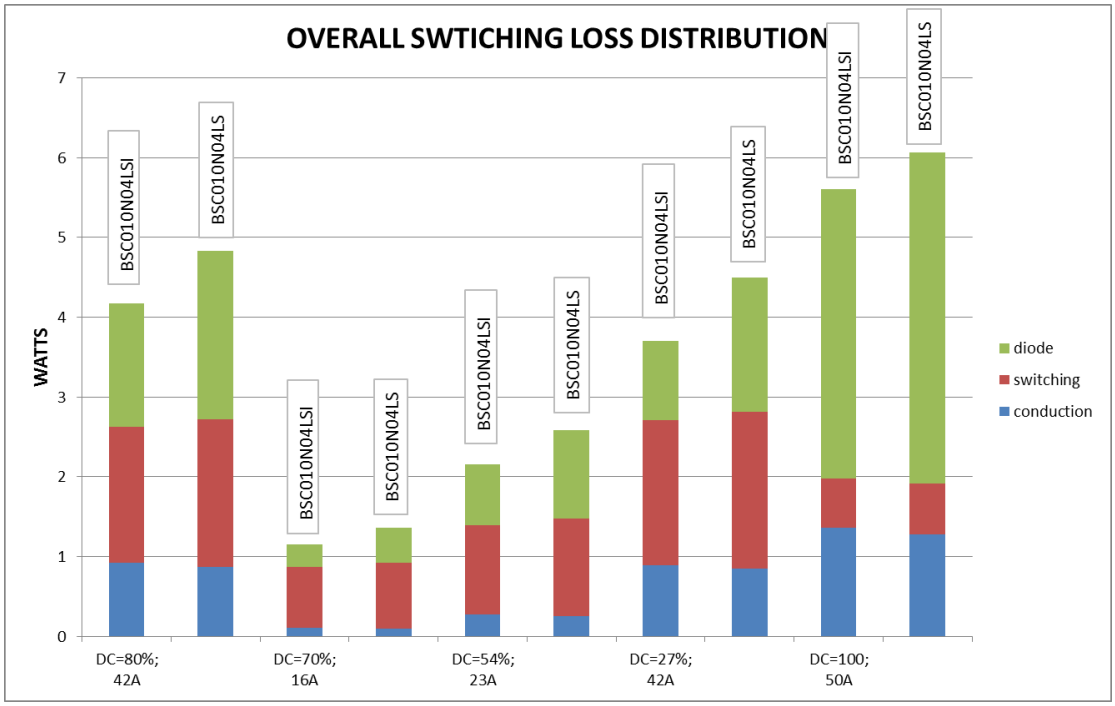

Figure 14: Absolute values

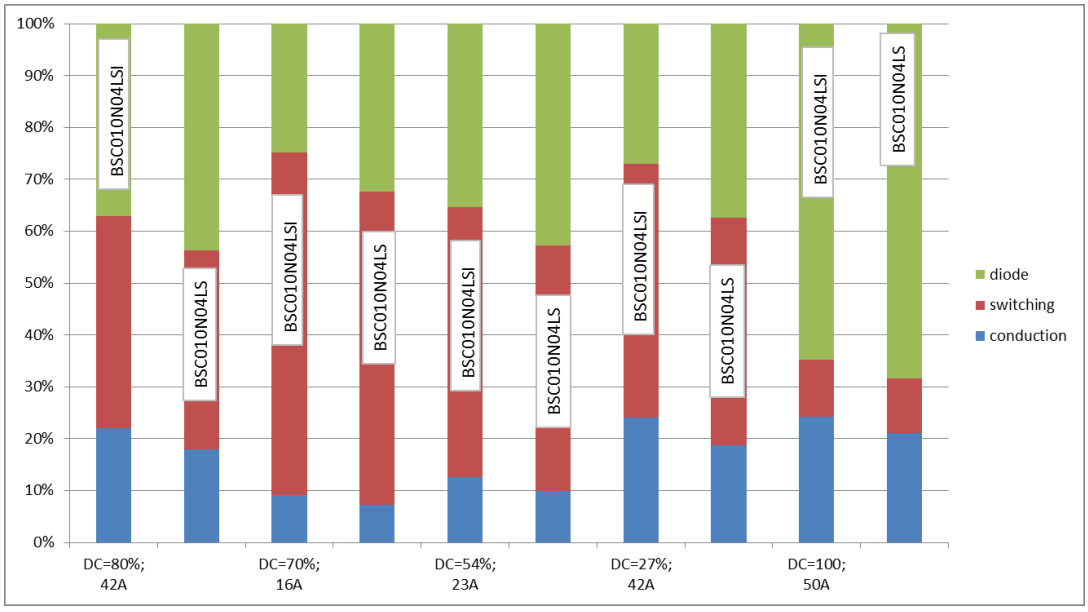

Figure 15: Normalized values

From the graph above we can see that the diode power loss is quite substantial, especially for 100% duty cycle at full power output.

If we compare a MOSFET with and without a Schottky-like diode we observe the difference as shown in figure 14. Note that Schottky-like diode parts are designated with the ending "…LSI"

From these results it is clear that the Schottky-like diode contributes to reduction of overall power losses.

The Infineon BSC010N04LSI has a slightly higher $R_{DS(on)}$ than the Infineon BSC010N04LS, which is also reflected in the slightly increased conduction loss. The switching loss remains the same, but the diode loss presents the biggest difference between these two elements.

From the bar graphs above we notice that switching losses are dominant for duty cycles <100%. This is also due to high gate resistance, but in the practical application designers must always find a fine balance between switching losses and voltage overshoots/ringing and EMI issues.

7 Practical calculation of power loss the Infineon way

The power loss results outlined above have been generated using a sophisticated and proprietary analysis tool that has been recently added to the portfolio of support solutions available to Infineon Technologies field application engineers (FAEs) to help them optimize their customers' designs. Unlike theoretical simulation tools that tend to deal with 'ideal' scenarios, the tool analyses real-life circuit data to deliver results that are directly applicable to the target application and that allow the engineer to make the best possible MOSFET selection.

In this case, all that is needed to start the power loss and optimization analysis process is a real-time oscilloscope capture of the phase current in one of the half bridges in the target inverter over one complete period (see Figure 16).

Figure 16: Real-time oscilloscope capture of phase current is starting point for power loss and optimization analysis

The information from this capture combined with other key data such as specific MOSFET characteristics, gate resistor values, dead time settings, frequencies, and pricing is fed into the Infineon tool, which can then quickly generate the power loss distribution, total power loss and performance/cost results.

8 Application Support

To help engineers reduce the time of evaluation, development, prototyping and testing Infineon has created a number of reference designs and demonstration boards for BLDC applications. Among these is a full plug and play system solution for a 1 kW cordless power drill as shown in Figure 17.

Figure 17: 1 kW BLDCM Full System Solution for Cordless Power Drill

This solution is built around the OptiMOS™ 5 40 V MOSFETs with integrated Schottky-like diode that we referred to earlier along with an Infineon EiceDRIVER™ gate driver and a 32-bit motor drive cost optimized XMC1302 host microcontroller. For increased safety of OEM batteries, an ORIGA™ chip hardware upgrade can be made which will be powered by already integrated ORIGA™ library in XMC™.

The power board itself measures just 4.5 cm x 3.6 cm x 1 cm, leading to a high power density of around 75 W/cm^3 and allowing the demo to easily be incorporated into existing power tools.

The design offers 1 kW of power and a peak current of over 200 A, and includes all of the hardware and software needed for implementation. In addition, for ease of use Infineon has designed the demo such that the PCB can be separated into three parts, namely Power PCB, Control PCB and Capacitor PCB.

Finally, as Figure 18 illustrates, it is worth noting that Infineon offers a variety of MOSFET options for battery-powered, low-frequency BLDC motor applications such as cordless power tools. These include the BiC OptiMOS™ 5 MOSFETs mentioned previously that offer voltage ratings from 20 V to 150 V, and 200 V to 300 V OptiMOS™ 3 devices. Furthermore Infineon customers have access to the StrongIRFET™ family of devices, which are optimized for low frequency and high rugged applications for voltages between 20 V and 200 V.

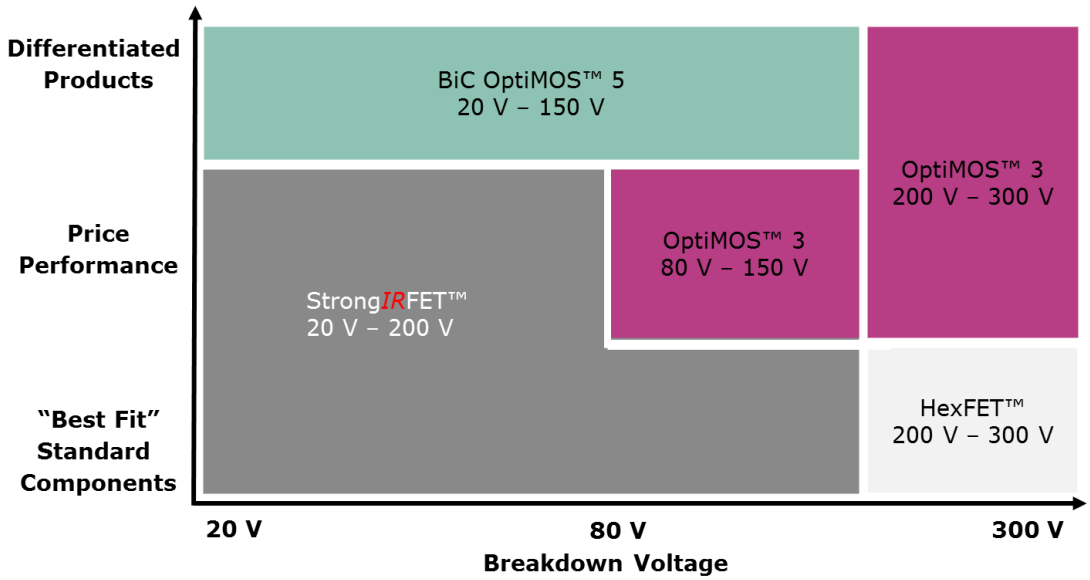

Figure 18: MOSFETs for battery-powered, low-frequency applications

9 References

Ref.1 Infineon Application note:

MOSFET Power Losses Calculation Using the Data-Sheet Parameters by Dr. Dusan Graovac Marco Puerschel,

Andreas Kiep

10 List of Figures

11 List of Tables

Published by
Infineon Technologies AG
85579 Neubiberg, Germany

Order Number: B111-I0282-V1-7600-EU-EC
Date: 04/ 2016